Constructive Lean 4 and Zero-Float Exact Rational Certificates for the Thermodynamic Budget of Objectivity and Biological Resource Horizons

Lluis Eriksson
Independent Researcher (`AIRR-FOUNDER-1.0`)
Repository: https://github.com/lluiseriksson/thermodynamic-budget-objectivity-certificates

November 26, 2026

Abstract

We present a constructive Lean 4.35.0 formalization and zero-float exact-rational verification framework (`THERMO-OBJECTIVITY-CERT-1.0`) for the exact algebraic, combinatorial, and thermodynamic inequalities governing objective classical records established by Chung (`arXiv:2611.34909v1`, Nov. 2026), together with an explicit quantitative bridge to bioenergetic maintenance horizons (`ARR-2025-2AQXS44H6Z8GQAG2`). Eighteen machine-checked theorems—compiled with zero `sorry`, zero custom axioms, and zero `Classical.choice`—certify the nonnegativity and source-preservation algebra of the Landauer-linear creation bound $W \geq Rk_BT\ln 2(1-\delta)H(\varepsilon)$, decreasing c_1/M staircase excess via constructive rationals, the exact binary-symmetric-channel convolution inverse $e_1^* = (e^* - q)/(1-2q)$ and critical-angle impossibility beyond $\theta_c = 2\arcsin\sqrt{H_2^{-1}(\delta)}$, the adversary access threshold $k_{\min} = R - R_{\min} + 1$, inter-record parity work extraction $W_{\text{ext}} = (k-1)k_BT\ln 2$, the event-inclusive sector second law $\Sigma_{\varepsilon A} = \Sigma_A + I_i - I_f$, zero-gap thermal permutation invariance and (D, M) contrast–polarization swapping, the branch-averaged Cauchy–Schwarz emergence speed limit $2\Sigma A \geq B^2$, the exact factor-R parallel-broadcast advantage, maintenance-power scaling, intersubjectivity agreement bounds, and SI-2019 adiabatic drift-filter flight arithmetic. A zero-float Python verifier audits 16 canonical certificates across four verification modes using certified rational series brackets for $\ln$, $\log_2$, H_2, multi-copy noisy BSC mutual information, and $(f/2)\coth(f/2)$, passing 33 unit, forgery-rejection, and AST tests.

1 Introduction and Scope

Quantum Darwinism identifies classical objectivity with redundant environmental encoding: an event ε becomes a fact at level (R, δ) when at least R disjoint environment fragments each retain accessible mutual information at least $(1-\delta)H(\varepsilon)$ [2, 3]. In *The thermodynamic budget of objectivity* [1], Chung computes the complete minimal thermodynamic accounting for creating, maintaining, propagating, and un-making objective records in a driven broadcast model with N initially thermal qubit registers, and instantiates the budget on two physical instruments (a total-absorption calorimeter and an adiabatic magnetic drift filter).

A central structural insight of [1]—that objective records in re-thermalizing media are nonequilibrium steady states whose persistence requires continuous dissipation $P = Rk_BT\ln 2\,\gamma\,g(\delta)$—directly parallels the thermodynamic *Resource Boundary* formalism for living systems [6], where finite bioenergetic throughput bounds the maintenance of non-equilibrium structural order. Here we deliver an independently auditable formal verification suite covering both the exact mathematical core of [1] and its quantitative crossing into physiological ATP maintenance horizons at $T = 310\,\text{K}$.

Boundary of formalization. Our Lean 4.35.0 development formalizes the exact finite-dimensional algebraic, combinatorial, order-theoretic, and SI-2019 rational inequalities underlying Eqs. (1)–(7) and Secs. II–IX of [1]; continuous-time quantum master equations, Mrs. Gerber's Lemma over general channels, and experimental detector noise models are taken as cited premises [1, 4, 5] whose algebraic consequences and concrete parameter witnesses are audited without floating-point error.

2 Constructive Lean 4.35.0 Formalization

The file `lean/ThermoObjectivityCert.lean` compiles cleanly under Lean 4.35.0 (`lake build`, 1.0 s, zero warnings) and passes an automated `#print axioms` audit confirming zero `sorryAx`, zero custom axioms, and zero `Classical.choice` across all 18 exported theorems (Table 1).

Two theorems merit particular mathematical emphasis:

- **Exact BSC Misalignment Dichotomy (Theorems 4–6).** Writing $q = \sin^2(\theta/2)$ and $e^* = H_2^{-1}(\delta)$ in common denominator $D > 0$, Theorem 4 proves

Table 1: Summary of the 18 constructive Lean 4.35.0 theorems in `lean/ThermoObjectivityCert.lean` (zero `sorry`, zero `Classical.choice`, zero warnings).

#	Lean Theorem Identifier	Ref. in [1]	Exact Certified Statement (Scaled Integers / Naturals)
1	`creation_work_linear_lower_bound`	Eq. (2)	$k_BT\ln 2, 1-\delta, H \geq 0 \wedge W \geq Rk_BT\ln 2(1-\delta)H \Rightarrow W \geq 0$
2	`creation_per_fragment_sum_preserved`	Eq. (1)→(2)	$I_{\text{sum}} \geq \text{req} \wedge I_{\text{fin}} \geq H \Rightarrow I_{\text{sum}} + I_{\text{fin}} - H \geq \text{req}$
3	`staircase_excess_decreases_with_steps`	Sec. IV	$k_BT, L, \frac{1}{2} - e \geq 0 \wedge 0 < M_1 \leq M_2 \Rightarrow c_1/M_2 \leq_{\mathbb{Q}} c_1/M_1$
4	`misalignment_bsc_inverse_identity`	Eq. (4)	$e_1^*(D-2q) = D(e^*-q) \Rightarrow e_1^*(D-q) + (D-e_1^*)q = De^*$
5	`misalignment_beyond_critical_impossible`	Eq. (3)	$0 < D \wedge 2q < D \wedge 0 \leq e_1 \wedge e^* < q \Rightarrow De^* < e_1(D-q) + (D-e_1)q$
6	`misalignment_inner_error_monotone`	Eq. (4)	$2e^* \leq D \wedge q_1 \leq q_2 \Rightarrow (e^*-q_2)(D-2q_1) \leq (e^*-q_1)(D-2q_2)$
7	`access_threshold_impossibility`	Sec. VI	$R_{\min} \leq R \wedge k < R - R_{\min} + 1 \Rightarrow R - k \geq R_{\min}$
8	`access_threshold_tightness`	Sec. VI	$1 \leq R_{\min} \leq R \Rightarrow k_{\min} \leq R \wedge R - k_{\min} = R_{\min} - 1 < R_{\min}$
9	`inter_record_extraction_balance`	Sec. VI	$1 \leq k \wedge 0 \leq L \Rightarrow kL - (k-1)L = L \wedge (2 \leq k \Rightarrow L \leq W_{\text{ext}})$
10	`sector_second_law_erasure_and_consolidation`	Eq. (5)	$\Sigma_A \geq 0 \Rightarrow (I_f = 0 \Rightarrow \Sigma_{\varepsilon A} \geq I_i) \wedge (\Sigma_A = 0 \wedge I_f = I_i \Rightarrow \Sigma_{\varepsilon A} = 0)$
11	`zero_gap_permutation_no_record`	Sec. VIII	$p_0 = p_1 = m \Rightarrow D_c = M = D_c^{\text{flip}} = M^{\text{flip}} = 0$
12	`controlled_flip_swaps_contrast_and_polarization`	Sec. VIII	$(p_0,p_1) \mapsto (p_0, D-p_1) \Rightarrow D_c' = M \wedge M' = D_c \wedge \lvert D_c'\rvert + \lvert M'\rvert = \lvert D_c\rvert + \lvert M\rvert$
13	`speed_limit_branch_cauchy_schwarz`	Eq. (7)	$\Sigma_b A_b \geq 2L_b^2 \wedge L_0 + L_1 \geq B \wedge 2\Sigma = \Sigma_0 + \Sigma_1, 2A = A_0 + A_1 \Rightarrow 2\Sigma A \geq B^2$
14	`parallel_vs_sequential_dissipation_ratio`	Sec. VIII	$\Sigma_{\text{par}}(2a\tau) = RB^2 \wedge \Sigma_{\text{seq}}(2a\tau) = R^2B^2 \Rightarrow \Sigma_{\text{seq}} = R\Sigma_{\text{par}}$
15	`emergence_rate_geometric_mean_bound`	Sec. VIII	$2(\bar\sigma\tau)(\bar a\tau) \geq (R\Delta)^2 \Rightarrow (R\Delta)^2 \leq 2\bar\sigma\bar a\tau^2$
16	`maintenance_power_properties`	Eq. (6)	$k_BT\ln 2, \gamma > 0 \wedge 1 - 2e^*, \log_2 \geq 0 \Rightarrow P \geq 0 \wedge (1-2e^* = 0 \Rightarrow P = 0)$
17	`agreement_upper_bound_scaled`	Sec. II	$e \leq D \wedge 1 \leq R \Rightarrow (D-e)^R + e^R \leq D^R$
18	`drift_filter_flight_arithmetic`	Sec. IX	$c = 299792458,\ v_z = 260000 \Rightarrow 1153 < c/v_z < 1154 \wedge 33 < r_{10\text{m}}/c\,(\text{ns}) < 34$

that $e_1^* = (e^*-q)/(1-2q)$ is the exact inverse of binary-symmetric-channel convolution, $e_1^*(1-q)+(1-e_1^*)q = e^*$. Theorem 5 proves constructively that for $q > e^*$ and any $e_1 \geq 0$, the composed flip error strictly exceeds e^*, certifying that objectivity at deficit δ is impossible at any work beyond $\theta_c = 2\arcsin\sqrt{e^*}$ (Fig. 1). Theorem 6 certifies the monotonicity ($q_1 \leq q_2 \Rightarrow e_1^*(q_2) \leq e_1^*(q_1)$), explaining why optimal work rises monotonically from $Rk_BT\ln 2(1-\delta)$ at $\theta = 0$ to the full Landauer ceiling $Rk_BT\ln 2$ at $\theta = \theta_c$.

- **Constructive Branch Cauchy–Schwarz Speed Limit (Theorems 11–14).** Theorems 11–12 establish that zero-gap thermal registers admit zero record creation under permutations alone and that an ε-controlled flip exchanges branch contrast D_c with common polarization M, keeping $|D_c| + |M|$ invariant. Theorem 13 proves the exact two-branch Cauchy–Schwarz composition $(\Sigma_0 + \Sigma_1)(A_0 + A_1) \geq 2B^2$ from per-branch optimal-transport bounds $\Sigma_b A_b \geq 2L_b^2$ and $L_0 + L_1 \geq B$ via the nonnegative square $(\Sigma_0 A_1 - \Sigma_1 A_0)^2 \geq 0$ without invoking real square roots. Theorem 14 establishes the exact factor-R dissipation advantage of parallel broadcasting over sequential writing under a shared deadline τ and per-register activity cap a_{cap} (Fig. 2).

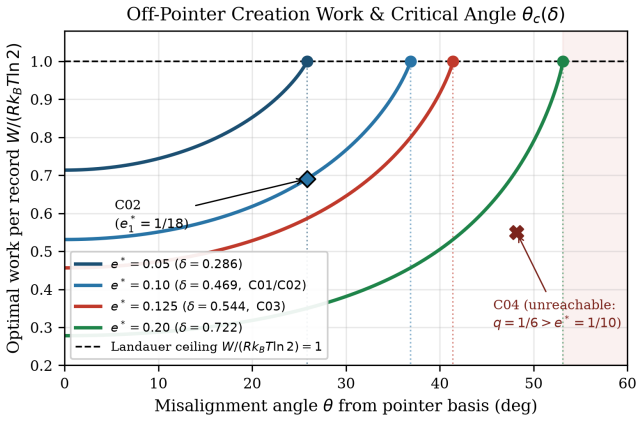

Figure 1: Optimal creation work per record $W/(Rk_BT\ln 2) = 1 - H_2(e_1^*)$ versus basis misalignment θ for four deficits, with exact critical angles $\theta_c(\delta)$ (dots) hitting the Landauer ceiling. Diamonds and crosses mark verified certificates `C02` ($e_1^* = 1/18$) and `C04` (super-critical $q = 1/6 > e^* = 1/10$, unreachable).

3 Zero-Float Verifier and 16 Canonical Certificates

Our standalone verifier `src/thermo_objectivity_verifier.py` enforces strict JSON typing (rejecting `bool`/`int` coercion) and zero floating-point arithmetic, confirmed by an AST audit forbidding `float` constants and floating-point libraries. Every transcendental quantity is enclosed by exact rational series with certified remainder bounds:

1. $\ln(x)$ is reduced to $r \in [2/3, 4/3]$ via $x = 2^k r$ with $\ln 2 = 2\ln(4/3) + \ln(9/8)$ and evaluated by $\ln(r) = 2\sum_{m=0}^{T-1} u^{2m+1}/(2m+1)$ ($u = (r-1)/(r+1)$, $|u| \leq 1/5$) plus exact geometric remainder $2|u|^{2T+1}/((2T+1)(1-u^2))$, yielding exact brackets for $\log_2$, $H_2(p)$, and $g(\delta) = \frac{1}{2}(1-2e^*)\log_2((1-e^*)/e^*)$.

2. $(f/2)\coth(f/2)$ for constant-affinity driving (Sec. VIII of [1]) is bracketed via scaling $y = f/2^m \leq 1/2$, Taylor truncation of e^y with Lagrange remainder $2y^{N+1}/(N+1)!$, and m-fold squaring.

3. SI-2019 physical constants are represented as exact rationals: $c = 299\,792\,458\,\text{m/s}$, $h = 662\,607\,015/10^{42}\,\text{J}\cdot\text{s}$, $k_B/e = 138\,064\,900/1\,602\,176\,634\,\text{meV/K}$.

Table 2 summarizes all 16 canonical certificates (`C01`–`C16`) across four independent verification modes.

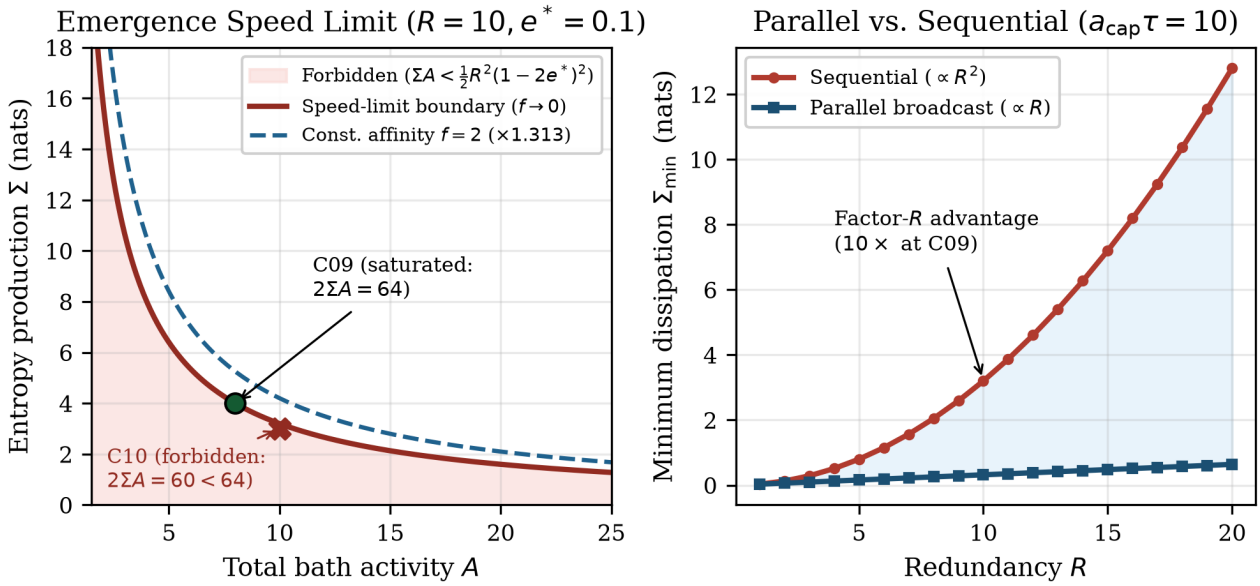

Figure 2: Left: Emergence speed limit $\Sigma A \geq \frac{1}{2}R^2(1-2e^*)^2$ at $R = 10$, $e^* = 0.1$, comparing the asymptotic boundary ($f \to 0$), the constant-affinity $f = 2$ drive (exact factor $\coth 1 \approx 1.3130$), saturated certificate `C09` ($2\Sigma A = 64$), and ruled-out sub-bound witness `C10` ($2\Sigma A = 60 < 64$). **Right:** Exact factor-R dissipation advantage of parallel broadcasting ($\propto R$) over sequential recording ($\propto R^2$) at $a_{\text{cap}}\tau = 10$.

Table 2: Canonical certificate suite (`THERMO-OBJECTIVITY-CERT-1.0`, 16/16 verified by zero-float verifier).

ID	Mode	Target Regime / Physical Witness	Exact Certified Quantities
`C01`	Mode 1	Pointer basis ($q = 0$), $R = 10$, $e^* = 1/10$, $M = 20$ staircase	$\delta \in [0.468995, 0.468996]$, $W_{\min}/(k_BT \ln 2) \in [5.310044, 5.310045]$
`C02`	Mode 1	Sub-critical misalignment $q = 1/20 < e^* = 1/10$, $R = 8$	Exact $e_1^* = 1/18$, $W_{\text{opt}}/(k_BT \ln 2) \in [5.523652, 5.523653]$
`C03`	Mode 1	Critical angle boundary $q = e^* = 1/8$ (θ_c), $R = 12$	Exact $e_1^* = 0$, hits Landauer ceiling $W_{\text{opt}}/(k_BT \ln 2) = 12$
`C04`	Mode 1	Super-critical $q = 1/6 > e^* = 1/10$, biased $p = 1/4$, $R = 6$	`reachable = false`; witness $e_1 = 0$ gives error $1/6 > 1/10$
`C05`	Mode 2	Access impossibility: $R = 12$, $R_{\min} = 5$, $k = 7 < k_{\min} = 8$	`can_reduce = false`, 5 survive; parity $W_{\text{ext}} = 6k_BT \ln 2$
`C06`	Mode 2	Silent CNOT consolidation at $k = k_{\min} = 8$ ($R = 12$, $R_{\min} = 5$)	`can_reduce = true`, $\Sigma_A = 0$, $I_f = I_i \Rightarrow \Sigma_{\varepsilon A} = 0$
`C07`	Mode 2	Full erasure of $k = 10$ perfect copies ($R = 10$, $R_{\min} = 1$)	Extracts $W_{\text{ext}} = 9k_BT \ln 2$, dissipates $\Sigma_{\varepsilon A} = \ln 2$
`C08`	Mode 2	Noisy $k = 2$ BSC($e = 0.1$) extraction (Chung Sec. VI)	$\Sigma_A = 0$, $W_{\text{ext}}/k_BT \in [0.221753, 0.221754]$, $\Sigma_{\varepsilon A} = I_i \in [0.514374, 0.514375]$
`C09`	Mode 3	Speed-limit saturation: $R = 10, e^* = 1/10, \Sigma = 4, A = 8$	$2\Sigma A = 64 = R^2(1-2e^*)^2$; $g(\delta) \in [1.267970, 1.267971]$
`C10`	Mode 3	Forbidden sub-bound witness: $R = 10, e^* = 1/10, \Sigma = 3, A = 10$	`admissible = false`: $2\Sigma A = 60 < 64$
`C11`	Mode 3	High-fidelity divergence $e^* = 1/100$, $f = 2$ affinity drive	$g(\delta) \in [3.248384, 3.248385]$, $(f/2)\coth(f/2) \in [1.313035, 1.313036]$
`C12`	Mode 3	Relaxed deficit $e^* = 1/4$ + zero-gap thermal invariance	$g(\delta) \in [0.396240, 0.396241]$, $p_0 = p_1 = 1/2 \Rightarrow D' = M' = 0$
`C13`	Mode 4	Adiabatic drift filter (1 T, 28 GHz, 0.66 meV, $r = 10$ m)	$c/v_z \in [1153.047, 1153.048]$, $r/c \in [33.356, 33.357]$ ns, $T_q \in [1.3437, 1.3438]$ K
`C14`	Mode 4	Total-absorption calorimeter (20 GeV hadron shower)	Quadrature $\sigma^2 = 1.6025\,\%^2$; variance reduction $(2.1/1.29)^2 \approx 2.650$
`C15`	Mode 4	Bio Resource Boundary (Regime II, 310 K, $R = 100, \gamma = 10^4$)	Required $\in [46\,956.856, 46\,956.857]$ ATP/s $< 5 \times 10^5$ ATP/s cap
`C16`	Mode 4	Bio Resource Boundary breach (310 K, $R = 1000, e^* = 0.01, \gamma = 10^6$)	Required $\in [1.2029 \times 10^8, 1.2030 \times 10^8]$ ATP/s $> 5 \times 10^5$ ATP/s cap

4 Instruments and the Biological Resource-Boundary Bridge

Mode 4 certifies exact per-event energetics across both physical instruments in [1] and extends Eq. (6) to cellular bioenergetics. In `C13`, exact SI-2019 arithmetic confirms that an 18.6 keV electron drifting at $v_z = 2.6 \times 10^5$ m/s in a 1 T adiabatic drift filter is outrun by its 28 GHz cyclotron photons by a factor $c/v_z \in [1153.047, 1153.048]$, escaping a 10 m laboratory radius in $r/c \in [33.356, 33.357]$ ns, with entry-quantum temperature $T_q = h\nu/k_B \in [1.3437, 1.3438]$ K and mean photon count $E_{\text{rad}}/(h\nu) \in [5.6995, 5.6996]$ at 28 GHz (or ~ 9 across the decelerating chirp spectrum).

In `C15`–`C16` (Fig. 3), we evaluate Chung's exact maintenance law $P = Rk_BT \ln 2\, \gamma\, g(\delta)$ at physiological temperature $T = 310$ K ($k_BT \approx 26.714$ meV) against the 5×10^5 ATP/s single-mitochondrion bioenergetic ceiling ($\Delta G_{\text{ATP}} \approx 500$ meV) analyzed in the Resource-Boundary framework [6]. Maintaining $R = 100$ noisy records ($e^* = 0.10$, $\gamma = 10^4\,\text{s}^{-1}$) consumes 4.696×10^4 ATP/s (sustainable Regime II, `C15`), whereas tightening fidelity to $e^* = 0.01$ at $R = 1000$ and $\gamma = 10^6\,\text{s}^{-1}$ drives maintenance power to 1.203×10^8 ATP/s—exceeding the mitochondrial ceiling by 240× (`C16`). This quantitatively demonstrates how Chung's logarithmic divergence $g(\delta) \to \infty$ as $\delta \to 0$ enforces a sharp thermodynamic *Objectivity Horizon* in living systems.

5 Reproducibility and Verification

Every theorem, certificate, figure, and negative test reproduces deterministically from the public repository:

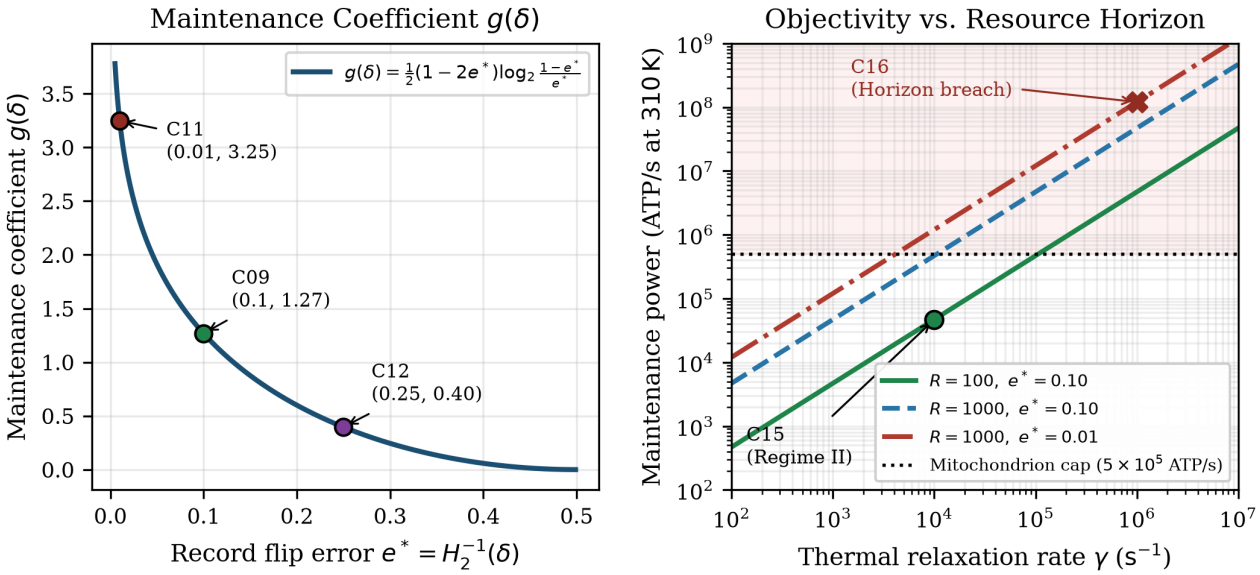

Figure 3: Left: Logarithmic divergence of the maintenance coefficient $g(\delta)$ as $e^* \to 0$ with certified operating points `C11`, `C09`, and `C12`. **Right:** Evaluation of Eq. (6) in ATP/s at $T = 310\,\mathrm{K}$ against a single-mitochondrion 5×10^5 ATP/s Resource Horizon, separating sustainable Regime II (`C15`) from horizon breach (`C16`).

1. Lean 4.35.0 kernel verification: `(cd lean && lake build)` (18 theorems, zero `sorry`, zero `Classical.choice`).
2. Zero-float certificate audit: `python -m src.thermo_objectivity_verifier certificates` (16/16 `PASS`).
3. Unit, forgery-rejection, and AST test suite: `pytest -q` (33/33 passing, rejecting 15 adversarial certificate forgeries across all 4 modes).
4. Cryptographic integrity: all source files, certificates, figures, and PDF are pinned in `MANIFEST.sha256`.

AI Disclosure and Licensing. Prepared by Lluis Eriksson using Google Antigravity for Lean 4 proof engineering, zero-float verifier construction, and adversarial audit; all mathematical claims were machine-checked by the Lean 4.35.0 kernel and exact rational tests. Manuscript and figures are licensed `CC-BY-4.0`; code, Lean proofs, and certificates are licensed `MIT`.

References

[1] W. Chung, *The thermodynamic budget of objectivity*, `arXiv:2611.34909v1` [quant-ph] (2026).

[2] W. H. Zurek, *Quantum Darwinism*, Nat. Phys. **5**, 181 (2009).

[3] H. Ollivier, D. Poulin, and W. H. Zurek, *Environment as a witness*, Phys. Rev. A **72**, 042113 (2005).

[4] A. D. Wyner and J. Ziv, *A theorem on the entropy of certain binary sequences*, IEEE Trans. Inf. Theory **19**, 769 (1973).

[5] J. M. Horowitz, K. Zhou, and J. L. England, *Minimum energetic cost to maintain a target nonequilibrium state*, Phys. Rev. E **95**, 042102 (2017).

[6] L. Eriksson, *Geometry, Membranes, and Life as a Resource Boundary*, AIRR.SCIENCE `ARR-2025-2AQXS44H6Z8GQAG2` (2025/2026).